

SUCCESSFUL CORONAL HEATING AND SOLAR WIND ACCELERATION BY MHD WAVES BY NUMERICAL SIMULATIONS FROM PHOTOSPHERE TO 0.3AU

Takeru K. Suzuki* & Shu-ichiro Inutsuka

Department of Physics, Kyoto University, Kitashirakawa, Kyoto, 606-8502, Japan; stakeru@scphys.kyoto-u.ac.jp

ABSTRACT

We show that the coronal heating and the acceleration of the fast solar wind in the coronal holes are natural consequence of the footpoint fluctuations of the magnetic fields at the photosphere by one-dimensional, time-dependent, and nonlinear magnetohydrodynamical simulation with radiative cooling and thermal conduction. We impose low-frequency ($< 0.05\text{Hz}$) transverse photospheric motions, corresponding to the granulations, with velocity $\langle dv_{\perp} \rangle = 0.7\text{km/s}$. In spite of the attenuation in the chromosphere by the reflection, the sufficient energy of the generated outgoing Alfvén waves transmit into the corona to heat and accelerate of the plasma by nonlinear dissipation. Our result clearly shows that the initial cool (10^4K) and static atmosphere is naturally heated up to 10^6K and accelerated to $\simeq 800\text{km/s}$, and explain recent SoHO observations and Interplanetary Scintillation measurements.

Key words: magnetic fields – plasma – magnetohydrodynamics – Sun : corona – solar wind – waves.

1. INTRODUCTION

It is still poorly understood how the coronal heating and the acceleration of the high-speed solar winds are accomplished in the open coronal holes which mainly exist in the polar regions except at the solar maximum phase. The origin of the energy to heat and accelerate the plasma is believed to be in the surface convection. This energy is lifted up through the magnetic fields and its dissipation leads to the plasma heating. In general, the problem of the coronal heating and the solar wind acceleration is to solve how the solar atmosphere reacts to the footpoint motions of the magnetic fields. Then, an ideal way to answer the problem is to solve the transfers of mass, momentum, and energy in a self-consistent manner from the photosphere to the interplanetary space, although such an attempt has not been successful yet.

In the coronal holes the Alfvén wave is regarded to play an important role (e.g. Belcher 1971), since it can travel a long distance to contribute not only to the coronal heating but to the solar wind acceleration. The Alfvén waves are excited by steady transverse motions of the field lines at the photosphere (e.g. Cranmer & van Ballegoijen 2005), while they can also be produced by continual reconnections above the photosphere (Axford & Mckee, 1997). The latter process might be responsible for generation of the high-frequency (up to 10^4Hz) ioncyclotron wave highlighted for the heating of the heavy ions (Kohl et al., 1998). However, it is difficult to sufficiently heat the protons having the higher resonant frequency by the high-frequency waves, because the wave energy is already absorbed by the heavy ions with higher mass-to-charge ratio (*i.e.* lower resonant frequency) (Cranmer, 2000). On the other hand, the low-frequency ($\lesssim 0.1\text{Hz}$) Alfvén wave does not have such a drawback; it can propagate a long distance and heat the bulk of the plasma. Since we focus on the heating of the major part of the plasma, we study the low-frequency Alfvén waves by the steady footpoint fluctuations.

The low-frequency Alfvén waves have been intensively studied in the context of the heating and acceleration of the solar wind plasma. For example, Oughton et al. (2001) and Dmitruk et al. (2002) examined turbulent cascade of the Alfvén waves in tangential directions. Recently, Ofman (2004) performed three-fluid and two-dimensional simulations for the wave-driven fast solar wind. These works are quite important in understanding the physical mechanism of the solar wind acceleration. One of the shortcomings of the previous research is that the most calculations for the wave-driven solar wind adopt the fixed ‘coronal base’, instead of the photosphere, as the inner boundary. In reality, however, the corona dynamically interacts with the chromosphere located below by chromospheric evaporation (Hammer, 1982) and wave transmission (Kudoh & Shibata, 1999) so that the coronal base varies time-dependently. Although some calculations (Lie-Svendsen et al., 2001, 2002) include the chromosphere and the transition region to properly take into account these effects, they assume unspecified mechanical energy deposition which requires an ad hoc heating function with the phenomenological dissipation length.

*JSPS Research Fellow

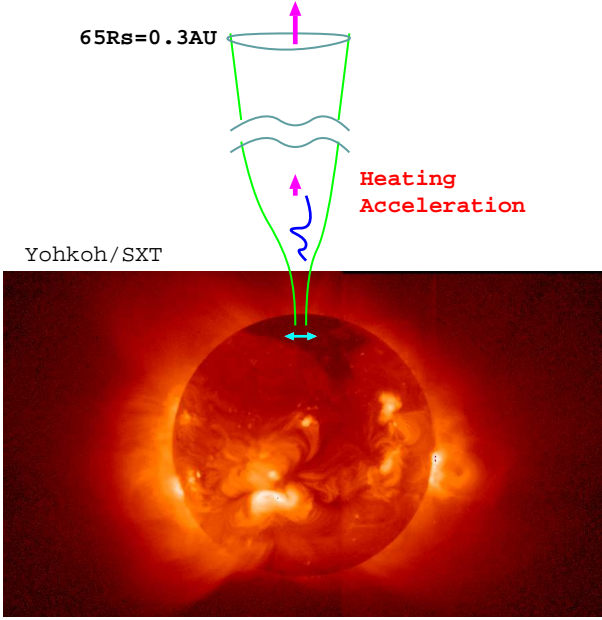


Figure 1. Schematic picture of our simulation (especially for NON-solar physicists). We consider the waves in the open flux tube rooted at the photosphere in the coronal hole to 0.3AU. Note that a coronal hole (dark region) is clearly seen in the north polar region in Yohkoh/SXT image.

In contrast, we self-consistently treat the transfer of the mass/momentum/energy by dynamically solving the wave propagation from the photosphere to the interplanetary region. We handle the heating and acceleration by the waves in an automatic way without the phenomenological heating function. Our aim is to answer the problem of the heating and acceleration in the coronal holes by the *forward* approach (Gudiksen & Nordlund, 2005) with the *minimal* unknown parameters.

2. SIMULATION METHOD

We consider one-dimensional open flux tube which is super-radially open (fig.1), measured by heliocentric distance, r . The simulation region is from the photosphere ($r = 1R_S$) with density, $\rho = 10^{-7} \text{ g cm}^{-3}$, to $65R_S$ (0.3AU), where R_S is solar radius. Radial field strength, B_r , is given by conservation of magnetic flux as

$$B_r r^2 f = \text{const.}, \quad (1)$$

where f is a super-radial expansion factor (Kopp & Orrall, 1976). In this paper B_r is set to be 161G at the photosphere, 5G at low coronal height, $r = 1.02R_S$, and $B_r = 2.1G(R_S/r)^2$ in $r > 1.5R_S$ by controlling f . We give transverse fluctuations of the field line by the granulations at the photosphere, which excite Alfvén waves. We consider the fluctuations with power spectrum, $P(\nu) \propto \nu^{-1}$, in frequency between

$6 \times 10^{-4} \leq \nu \leq 0.05 \text{ Hz}$ (period of 20seconds — 30minutes), and root mean squared (rms) average amplitude $\langle dv_{\perp} \rangle \simeq 0.7 \text{ km/s}$ corresponding to observed velocity amplitude $\sim 1 \text{ km/s}$ (Holweger, Gehlsen, & Ruland, 1978). At the outer boundary, non-reflecting condition is imposed for all the MHD waves (Suzuki & Inutsuka, 2005a,b), which enables us to carry out simulations for a long time until quasi-steady state behaviors are achieved without unphysical wave reflection.

We dynamically treat propagation and dissipation of the waves and heating and acceleration of the plasma by solving ideal MHD equations with the relevant physical processes :

$$\rho \frac{d}{dt} \left(\frac{1}{\rho} \right) - \frac{1}{r^2 f} \frac{\partial}{\partial r} (r^2 f v_r) = 0, \quad (2)$$

$$\begin{aligned} \rho \frac{dv_r}{dt} = & -\frac{\partial p}{\partial r} - \frac{1}{8\pi r^2 f} \frac{\partial}{\partial r} (r^2 f B_{\perp}^2) \\ & + \frac{\rho v_{\perp}^2}{2r^2 f} \frac{\partial}{\partial r} (r^2 f) - \rho \frac{GM_S}{r^2}, \end{aligned} \quad (3)$$

$$\rho \frac{d}{dt} (r \sqrt{f} v_{\perp}) = \frac{B_r}{4\pi} \frac{\partial}{\partial r} (r \sqrt{f} B_{\perp}), \quad (4)$$

$$\begin{aligned} \rho \frac{d}{dt} \left(e + \frac{v^2}{2} + \frac{B^2}{8\pi\rho} - \frac{GM_{\odot}}{r} \right) + \frac{1}{r^2 f} \frac{\partial}{\partial r} [r^2 f \{ (p + \frac{B^2}{8\pi}) v_r - \frac{B_r}{4\pi} (\mathbf{B} \cdot \mathbf{v}) \}] \\ + \frac{1}{r^2 f} \frac{\partial}{\partial r} (r^2 f F_c) + q_R = 0, \end{aligned} \quad (5)$$

$$\frac{\partial B_{\perp}}{\partial t} = \frac{1}{r \sqrt{f}} \frac{\partial}{\partial r} [r \sqrt{f} (v_{\perp} B_r - v_r B_{\perp})], \quad (6)$$

where ρ , \mathbf{v} , p , e , \mathbf{B} are density, velocity, pressure, specific energy, and magnetic field strength, respectively, and subscript r and \perp denote radial and tangential components. G and M_S are the gravitational constant and the solar mass. F_c is thermal conductive flux and q_R is radiative cooling (Landini & Monsignori-Fossi, 1990; Anderson & Athay, 1989; Moriyasu et al., 2004). We adopt 2nd-order MHD-Godunov-MOCCT scheme for updating the physical quantities (Sano & Inutsuka 2005), of which an advantage is that no artificial viscosity is required even for strong MHD shocks. We fix 14000 grid points with variable sizes in a way to resolve Alfvén waves with $\nu = 0.05 \text{ Hz}$ by at least 10 grids per wavelength to reduce numerical damping.

The advantages of our simulation are (i) automatically treating wave propagation/dissipation and plasma heating/acceleration without an ad hoc heating function (ii) with minimal assumption, *i.e.*, the transverse footpoint motions in the given flux tube (iii) in the broadest regions with respect to the density contrast amounting to 15 orders of magnitude from the photosphere to 0.3AU. On the other hand, the disadvantages are due to the 1-dimensional MHD approximation; we assume that the wave propagation is restricted to the direction parallel to the field line and the plasma behaves as the one-fluid with the Boltzmann particle distribution. We will discuss this issues later. We would like to emphasize however, that this is the most self-consistent simulation for the solar wind acceleration, in spite of these shortcomings.

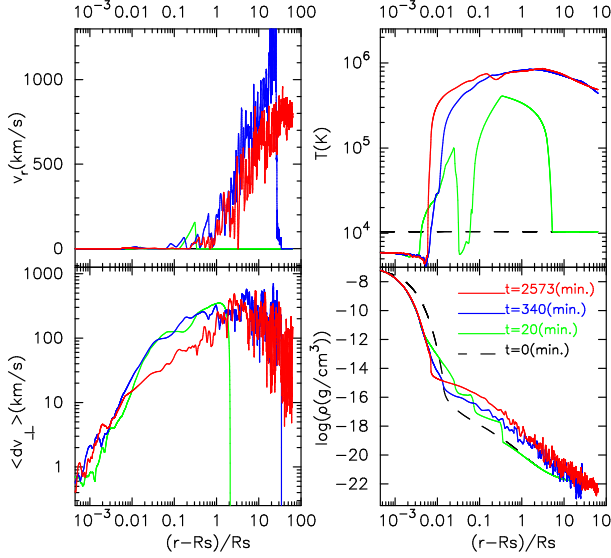


Figure 2. Time evolution of the atmosphere. Outflow speed, v_r (km/s) (upper-left), temperature, T (K) (upper-right), density, rms amplitude of transverse velocity, $\langle dv_{\perp} \rangle$ (km/s) (lower-left), and ρ (g/cm³) (lower-right) are plotted. Black dashed, green, blue, and red solid lines are results at $t = 0, 20, 340$, & 2573 mins., respectively, whereas results at $t = 0$ do not appear in $\langle dv_{\perp} \rangle$ because it equals to 0. The results are averaged by integrating for 3 minutes to take into account effects of the exposure time for comparison with observations.

3. RESULTS

We initially set static and cool atmosphere with temperature, $T = 10^4$ K; we do not impose the corona and the solar wind at the beginning. Figure 2¹ shows how the coronal heating and the solar wind acceleration are realized by the generated low-frequency Alfvén waves. We plot v_r (km/s), T (K), ρ (g/cm³), and $\langle dv_{\perp} \rangle$ (km/s) averaged from v_{\perp} as a function of $(r - R_s)/R_s$ at different time, $t = 0, 20, 340$ & 2573 minutes. As time goes on, the atmosphere is heated and accelerated effectively by dissipation of the Alfvén waves. Temperature rises rapidly in the inner region even at $t = 20$ minutes, and the outer region is eventually heated up by both outward thermal conduction and wave dissipation. Once the plasma is heated up to the coronal temperature, mass is supplied to the corona mainly by chromospheric evaporation due to the downward thermal conduction. This is seen in temperature structure as an inward shift of the transition region, which is finally located around $r = 6 \times 10^{-3} R_s$ ($\simeq 4000$ km), whereas it moves up and down by the time-dependent chromospheric evaporation (heating) and the wave transmission. As a result, the coronal density increases by two orders of magnitude. While the wind velocity exceeds 1000 km/s at $t = 340$ minutes on account of the initial low density, it gradually settles down to

< 1000 km/s as the density increases. $\langle dv_{\perp} \rangle$ also settles down to the reasonable value at the final stage. Temperature structure is smoother owing to the thermal conduction than the other quantities showing fluctuated behaviors due to the waves.

We have found that the plasma is steadily heated up to 10^6 K in the corona and flows out as transonic wind with $v_r \simeq 800$ km/s at the outer boundary ($= 0.3$ AU) when the quasi steady-state behaviors are achieved after $t \gtrsim 1800$ minutes. This is the first numerical simulation which directly shows that the heated plasma actually flows out as the transonic wind, initiated from the static and cool atmosphere, by the Alfvén waves. The outflow speed becomes up to 10 km/s even below 10^4 km above the photosphere (c.f. Tu et al. 2005), although it is difficult to distinguish from the longitudinal wave motions. The sonic point where v_r exceeds the local sound speed is located at $r \simeq 2.5 R_s$ and the Alfvén point is at $r \simeq 24 R_s$. Obtained proton flux at 0.3 AU is $N_p v \simeq (2 \pm 0.5) \times 10^9$ (cm⁻²s⁻¹), corresponding to $N_p v \simeq (1.8 \pm 0.5) \times 10^8$ (cm⁻²s⁻¹) at 1 AU for $N_p v \propto r^{-2}$, which is consistent with the observed high-speed stream around the earth (Aschwanden, Poland, & Robin, 2001).

In fig. 3 we compare the result at $t = 2573$ minutes with recent observation in the high-speed solar winds from the polar regions by Solar & Heliospheric Observatory (SoHO) (Zangrilli et al., 2002; Teriaca et al., 2003; Fludra, Del Zanna, & Bromage, 1999; Lamy et al., 1997; Wilhelm et al., 1998; Banerjee et al., 1998; Esser et al., 1999) and Interplanetary Scintillation (IPS) measurements (Grall et al., 1996; Kojima et al., 2004; Canals et al., 2002). The figure shows that our forward simulation naturally form the corona and the high-speed solar wind which are observed except small differences in detailed structures. Observed outflow speed in the inner corona ($\leq 3 R_s$) and outer region ($\gtrsim 20 R_s$) are mostly explained by our simulation within the observed errors. Some of the observed data around $r \simeq 10 R_s$ (Grall et al., 1996) exceed our result, whereas it is reported that these data might reflect wave phenomena rather than the outflow speed (Harmon & Coles, 2005). The simulated temperature shows a decent agreement with the electron temperature in the inner region by SoHO (Fludra et al. 1997). Density and transverse amplitude show reasonable agreements with the observations.

Our result manifestly shows that the heating and acceleration of the high-speed winds from the open field regions can be almost completely explained by the MHD dissipation mechanisms of the low-frequency Alfvén waves. The result is quite convincing since we automatically solve the transfers of mass/momentum/energy and the propagation of the Alfvén waves excited at the photosphere without any ad hoc assumptions.

Figure 4 presents energy flux of outgoing Alfvén wave, incoming Alfvén wave, and outgoing MHD slow (sound) wave at $t = 2573$ minutes. To focus on the amount of dissipation the energy flux is normalized by the cross section

¹Movie file is available :

http://www-tap.scphys.kyoto-u.ac.jp/~stakeru/research/suzuki_200506.mpg

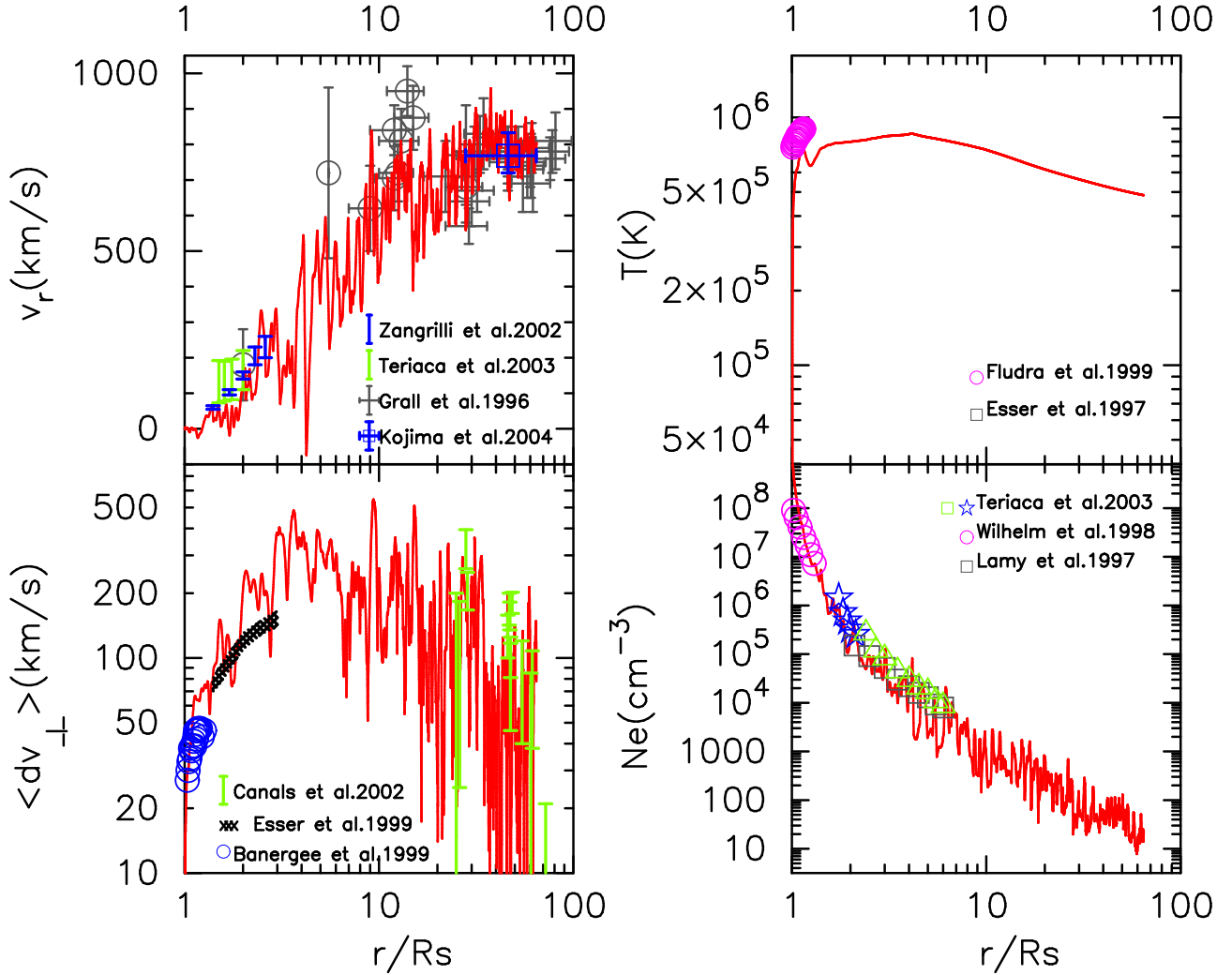


Figure 3. Comparison of the result at $t = 2573$ mins (red solid lines) with observations summarized below. Quantities in four panels are the same as in fig.2 except lower-right panel showing electron density, $N_e(\text{cm}^{-3})$, instead of $\rho(\text{g cm}^{-3})$. Scales in both horizontal and vertical axes are changed from fig.2. **a:** Vertical error bars with green x's (Teriaca et al., 2003) and blue triangles (Zangrilli et al., 2002) are proton outflow speed in polar regions by SoHO. Blue square with errors is velocity by IPS measurements averaged in 0.13 - 0.3AU of high-latitude regions(Kojima et al., 2004). Crossed bars with and without circles are measurements by VLBI and IPS(EISCAT) (Grall et al., 1996). Vertical error bars with circles are data based on observation by SPARTAN 201-01 (Habbal et al., 1995). **b:** Pink circles are electron temperature by CDS/SoHO (Fludra, Del Zanna, & Bromage, 1999). **c:** Pink circles and blue stars are observations by SUMER/SoHO (Wilhelm et al., 1998) and by CDS/SoHO (Teriaca et al., 2003), respectively. Green triangles (Teriaca et al., 2003) and squares (Lamy et al., 1997) are observations by LASCO/SoHO. **d:** Blue circles are non-thermal broadening inferred from SUMER/SoHO measurements (Banerjee et al., 1998). Cross hatched region is empirically derived non-thermal broadening based on UVCS/SoHO observation (Esser et al., 1999). Green error bars with circles are transverse velocity fluctuations derived from IPS measurements by EISCAT (Canals et al., 2002).

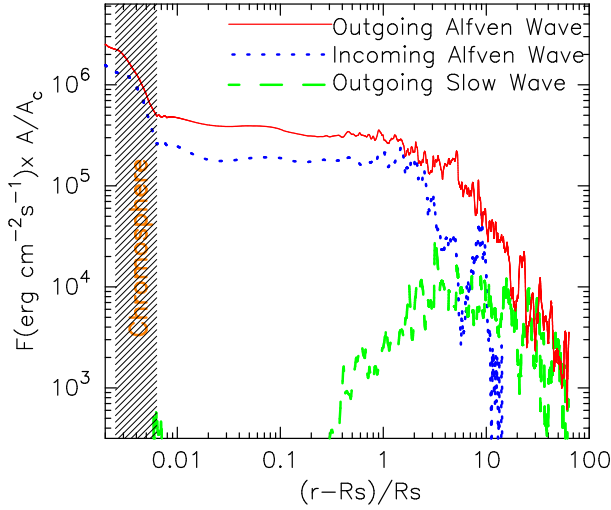


Figure 4. Energy flux of outgoing Alfvén (red solid), incoming Alfvén (blue dotted), and outgoing MHD slow (green dashed) waves at $t = 2573$ mins. Hatched region indicates the chromosphere. The energy flux is normalized by the cross section ($A = r^2 f$) of the flux tube at $r = 1.02R_S$ and A_c denotes A at that location.

of the flux tube at $r = 1.02R_S$ where it expands super-radially by 30 times from the photosphere. Note that the real energy flux in the lower (upper) regions is larger (smaller). The outgoing and incoming Alfvén waves are decomposed by correlation between v_\perp and B_\perp (Elsässer variables). Extraction of the slow wave is also from fluctuating components of v_r and ρ . The derived energy flux is averaged by integrating for 30 minutes to smooth out variation due to phase.

The figure shows that the outgoing Alfvén wave dissipate quite effectively; less than 10^{-3} of the initial energy is remained as that associated with the waves at the outer boundary. First, a sizable amount is reflected back downward below the coronal base ($r - R_S < 0.01R_S$), which is clearly illustrated in the energy flux of the incoming Alfvén wave following that of the outgoing component with slightly smaller level. This is because the wave shape is considerably deformed owing to the steep density gradient; a typical variation scale ($< 10^5$ km) of the Alfvén speed becomes comparable or even shorter than the wavelength ($= 10^4 - 10^6$ km). Although the energy flux, $\simeq 5 \times 10^5 \text{ erg cm}^{-2} \text{ s}^{-1}$, of the outgoing Alfvén waves which penetrates into the corona is only $\simeq 15\%$ of the input value, it meets the requirement for the energy budget in the coronal holes (Withbroe & Noyes, 1977).

Second, MHD slow (sound) waves (Sakurai et al., 2002) are generated in the corona as shown in the figure. The amplitude of the Alfvén waves is amplified through the upward propagation, as a result, a nonlinear term due to variation of magnetic pressure accompanying with the Alfvén waves excites longitudinal slow waves (Kudoh & Shibata, 1999). They eventually steepen to form MHD slow shocks (Suzuki, 2002)

which efficiently convert kinetic and magnetic energy to heat. The coronal heating and wind acceleration are thus far achieved by transfer from the energy and momentum of the outgoing Alfvén waves. Linearly polarized Alfvén waves directly steepen in themselves to form MHD fast shocks (Hollweg, 1982; Suzuki, 2004), which also contributes to the heating, though it is less dominant. The incoming Alfvén waves are generated in the corona by the reflection of the outgoing ones by the density fluctuations due to the slow waves. The reflected waves further play a role in the dissipation of the outgoing Alfvén waves by nonlinear wave-wave interaction.

4. SUMMARY AND DISCUSSIONS

We have performed one-dimensional MHD simulation for the low-frequency Alfvén waves excited at the photosphere. We incorporate radiative cooling and thermal conduction, and self-consistently treat the mass, momentum, and energy transfer by nonlinearly and dynamically solving the wave propagation and dissipation. The advantage of our simulation is the *forward* approach with the *minimal* assumptions.

Our result has manifestly shown that the formation of the corona and the acceleration of the fast solar wind in the coronal holes are the natural outcome of the footpoint motions of the field line. The photospheric fluctuations generate the low-frequency Alfvén waves which propagate upwardly. About 15% of the initial Alfvén waves in energy flux can transmit into the corona after surviving the non-WKB reflection in the chromosphere and the transition region. The amplitudes of these out-going waves are amplified due to the density stratification so that they effectively dissipate by the nonlinear effects and heat and accelerate the coronal plasma.

A key mechanism in the coronal heating and the solar wind acceleration is the generation of the MHD slow wave. Thus, one of the predictions from our simulation is the existence of the longitudinal fluctuations in the solar wind plasma. This is directly testable by future missions, Solar Orbiter and Solar Probe, which will approach to ~ 45 and $4 R_S$, respectively, being in our simulation region. They can determine how much fractions of the fluctuations are in the transverse and longitudinal modes by in situ measurements which are directly compared with our result.

In this paper we have considered the wave propagation and dissipation in one-dimensional MHD approximation. However, its validity needs to be examined by future studies. It is important to investigate the multidimensional effects for the waves (Ofman, 2004), such as refraction (Bogdan et al., 2003), phase mixing (Heyvaerts & Priest, 1983; Nakariakov, Roberts, & Murawski, 1998), turbulent cascade into the transverse direction (Oughton et al., 2001; Dmitruk et al., 2002). The waves could suffer collisionless damping (e.g. Suzuki et al. 2005), and

this mechanism might also modify the dissipation rate. Kinetic effects of the multicomponent plasma might be also important especially in the outer region with low density.

We need to check how much the wave dissipation and the consequent plasma heating are modified by these processes. However, we cannot study them in the global simulations as performed here because of the huge density difference. Hence, we should firstly investigate the detailed processes in the local simulations, and then, compare with global results; the global simulation in the one-dimension and the local simulations in the two- or three-dimensions should play complimentary roles.

ACKNOWLEDGMENT

We thank Drs. K. Shibata and T. Sano for many fruitful discussions. T.K.S. is supported by the JSPS Research Fellowship for Young Scientists, grant 4607. This work is supported by the Grant-in-Aid for the 21st Century COE "Center for Diversity and Universality in Physics" at Kyoto University from the Ministry of Education, Culture, Sports, Science and Technology (MEXT) of Japan.

REFERENCES

- Anderson, C. S. & Athay, R. G. 1989, ApJ, 336, 1089
- Aschwanden, M. J., Poland, A. I., & Robin, D. M. 2001, ARA&A, 39, 175
- Axford, W. I. & McKenzie, J. F. 1997, *The solar wind. Cosmic Winds and the Heliosphere*, (Eds.) Jokipii, J. R., Sonnet, C. P., and Giampapa, M. S., University of Arizona Press
- Banerjee, D., Teriaca, L., Doyle, J. G., & Wilhelm, K. 1998, A&A, 339, 208
- Belcher, J. W. ApJ, 168, 509
- Bogdan, T. J. et al. 2003, ApJ, 500, 626
- Canals, A., Breesn, A. R., Ofman, L., Moran, P. J., & Fallows, R. A. 2002, Ann. Geophys. 20, 1265
- Cranmer, S. R. 2000, ApJ, 532, 1197
- Cranmer, S. R. & van Ballegoijen, A. A. 2003, ApJ, 594, 573
- Dmitruk, P., Matthaeus, W. H., Milano, L. J., Oughton, S., Zank, G. P., & Mullan, D. J. 2002, ApJ, 575, 571
- Esser, R., Fineschi, S., Dobrzycka, D., Habbal, S. R., Edgar, R. J., Raymond, J. C., & Kohl, J. L. 1999, ApJL, 510, L63
- Fludra, A., Del Zanna, G. & Bromage, B. J. I. 1999, Spac. Sci. Rev., 87, 185
- Grall, R. R. et al., Coles, W. A., Klinglesmith, M. T., Breen, A. R., Williams, P. J. S., Markkanen, J., & Esser, R. 1996, Nature, 379, 429
- Gudiksen, B. V. & Nordlund, Å. 2005, ApJ, 618, 1020
- Habbal, S. R., Esser, R., Guhathakura, M., & Fisher, R. R. 1995, Geophys. Res. Lett., 22, 1465
- Hammer, R. 1982, ApJ, 259, 767
- Harmon, J., K. & Coles, W., A. 2005, JGR, 110, A03101
- Heyvaerts, J. & Priest, E. R. 1983, A&A, 117, 220
- Hollweg, J. V. 1982, ApJ, 254, 806
- Holweger, H., Gehlsen, M., & Ruland, F. 1978, A&A, 70, 537
- Kohl, J. L. et al. 1998, ApJL, 501, L127
- Kojima, M. et al. 2004, JGR, 109, A04103
- Kopp, R. A. & Orrall, F. Q. 1976, A&A, 53, 363
- Kudoh, T. & Shibata, K. 1999, ApJ, 514, 493
- Lamy, P. et al. 1981, *Fifth SOHO Workshop, The Corona and Solar Wind near Minimum Activity*, (ed) A. Wilson (ESA-SP 404; Noordwijk:ESA), 491
- Landini, M. & Monsignori-Fossi, B. C. 1990, A&AS, 82, 229
- Lie-Svendsen, Ø, Hansteen, V. H., & Leer, E. 2002, JGR, 106, 8217
- Lie-Svendsen, Ø, Hansteen, V. H., Leer, & E. Holzer, T. E. 2002, ApJ, 566, 562
- Moriyasu, S., Kudoh, T., Yokoyama, T., & Shibata, K. 2004, ApJ, 601, L107
- Nakariakov, V. M., Roberts, B., & Murawski, K. 1998, A&A, 332, 795
- Ofman, L. 2004, JGR, 109, A07102
- Oughton, S. et al., Matthaeus, W. H., Dmitruk, P., Milano, L. J., Zank, G. P., & Mullan, D. J. 2001, ApJ, 551, 565
- Sakurai, T., Ichimoto, K., Raju, K. P., & Singh, J. Sol.Phys., 209, 265
- Sano, T. & Inutsuka, S. 2005, in preparation
- Suzuki, T. K. 2002, ApJ, 578, 598
- Suzuki, T. K. 2004, MNRAS, 349, 1227
- Suzuki, T. K., Yan, H., Lazarian, A. & Cassinelli, J. P. 2005, Submitted to ApJ (astro-ph/0505013)
- Suzuki, T. K. & Inutsuka, S. 2005a, ApJL in press (astro-ph/0506639)
- Suzuki, T. K. & Inutsuka, S. 2005b, in preparation
- Teriaca, L., Poletto, G., Romoli, M., & Biesecker, D. A. 2003, ApJ, 588, 566
- Tu, C.-Y., Zhou, C., Marsch, E., Xia, L.-D., Zhao, L., Wang, J.-X., & Wilhelm, K. 2005, Science, 308, 519
- Wilhelm, K., Marsch, E., Dwivedi, B. N., Hassler, D. M., Lemaire, P., Gabriel, A. H., & Huber, M. C. E. 1998, ApJ, 500, 1023
- Withbroe, G. L. & Noyes, R. W. 1977, ARA&A, 15, 363
- Zangrilli, L., Poletto, G., Nicolosi, P., Noci, G., & Romoli, M. 2002, ApJ, 574, 477